Molecular Systems Biology 5; Article number 259; doi:10.1038/msb.2009.18
Citation: ***Molecular Systems Biology*** **5:259**

www.molecularsystemsbiology.com

molecular systems biology

Metabolomics of the interaction between PPAR-α and age in the PPAR-α-null mouse

Helen J Atherton[1], Melanie K Gulston[1], Nigel J Bailey[2], Kian-Kai Cheng[1], Wen Zhang[3], Kieran Clarke[3] and Julian L Griffin[1,4,*]

[1] Department of Biochemistry & Cambridge Systems Biology Centre, University of Cambridge, Cambridge, UK, [2] Selcia Ltd, Fyfield Business and Research Park, Ongar, Essex, UK, [3] University Laboratory of Physiology, University of Oxford, Oxford, UK and [4] Metabolic Research Laboratory, Institute of Metabolic Sciences, University of Cambridge, Addenbrooke's Hospital, Cambridge, UK

* Corresponding author. Department of Biochemistry, University of Cambridge, Tennis Court Road, Cambridge CB2 1QW, UK. Tel.: +44 1223 764 922; Fax: +44 1223 766 002; E-mail: jlg40@mole.bio.cam.ac.uk

Received 9.10.08; accepted 10.2.09

Regulation between the fed and fasted states in mammals is partially controlled by peroxisome proliferator-activated receptor-α (PPAR-α). Expression of the receptor is high in the liver, heart and skeletal muscle, but decreases with age. A combined ^{1}H nuclear magnetic resonance (NMR) spectroscopy and gas chromatography-mass spectrometry metabolomic approach has been used to examine metabolism in the liver, heart, skeletal muscle and adipose tissue in PPAR-α-null mice and wild-type controls during ageing between 3 and 13 months. For the PPAR-α-null mouse, multivariate statistics highlighted hepatic steatosis, reductions in the concentrations of glucose and glycogen in both the liver and muscle tissue, and profound changes in lipid metabolism in each tissue, reflecting known expression targets of the PPAR-α receptor. Hepatic glycogen and glucose also decreased with age for both genotypes. These findings indicate the development of age-related hepatic steatosis in the PPAR-α-null mouse, with the normal metabolic changes associated with ageing exacerbating changes associated with genotype. Furthermore, the combined metabolomic and multivariate statistics approach provides a robust method for examining the interaction between age and genotype.
Molecular Systems Biology 7 April 2009; doi:10.1038/msb.2009.18
Subject Categories: cellular metabolism
Keywords: functional genomics; hepatic steatosis; metabonomics; obesity

Introduction

Fatty acids are able to stimulate their own catabolism through a set of nuclear receptors called the peroxisome proliferator-activated receptors (PPARs) (Keller *et al*, 1993), which control the expression of a variety of genes involved in lipid metabolism and energy homoeostasis (Dreyer *et al*, 1992; Motojima *et al*, 1998; Berger and Moller, 2002). Of the three PPAR isoforms that exist (PPAR-α, PPAR-δ and PPAR-γ), fatty acids bind to PPAR-α with the greatest affinity (Desvergne and Wahli, 1999). PPAR-α is highly expressed in tissues with a high catabolic rate such as the liver, kidneys, heart and skeletal muscle (Braissant *et al*, 1996) and its activation results in downstream transcription of genes controlling fatty acid transport, uptake, intracellular binding and catabolism (Issemann *et al*, 1992). PPAR-α is also activated by fibrates, a synthetic class of compounds that improve muscle and hepatic insulin resistance, decrease the fat content of the liver and reduce the circulating levels of non-esterified fatty acids (NEFAs) in both rodents and humans (Guerre-Millo *et al*, 2000; Rubins *et al*, 2002).

Although the role of PPAR-α in regulating the transition between the fed and fasted states, particularly in the liver, has been widely investigated, its role in normal ageing has been much less studied. However, PPAR-α expression is known to decrease in a range of tissues including the liver and heart with age (Iemitsu *et al*, 2002; Sanguino *et al*, 2005; Ye *et al*, 2005).

The PPAR-α-null mouse (Lee *et al*, 1995) has considerably aided research into the role of this receptor. The loss of PPAR-α function results in increased circulating triacylglyceride concentrations and fatty infiltration of the liver (Peters *et al*, 1997; Barak and Kim, 2007). However, most previous studies have detected only these changes in the PPAR-α-null mouse during fasting (Kersten *et al*, 1999; Leone *et al*, 1999), when the mice develop profound hypoglycaemia and severe lipid accumulation in organs including the heart and liver (Djouadi *et al*, 1998). The ketogenic response to low nutrient levels is also lacking, resulting in insufficient delivery of energy supply

to peripheral tissues (Leone *et al*, 1999). All these perturbations are documented to be secondary to an underlying defect in fatty acid oxidation, which results from an inability to increase β-oxidation under conditions of low glucose uptake, ultimately leading to the observed energy deficits in this mouse (Le May *et al*, 2000). In contrast to these studies that focus on animals under fasted conditions, we have previously detected profound perturbations in glycolysis, gluconeogenesis, amino-acid metabolism and fatty acid metabolism in a range of tissues in the PPAR-α-null mouse at 1 month when fed *ad libitum* using a metabolomic-based approach (Atherton *et al*, 2006). Metabolomics describes the comprehensive analysis of the collection of small molecule metabolites associated with a cell, tissue, organ or organism in a context-dependent manner (Weckwerth, 2003; Griffin, 2004), and has been discriminatory even for mild or 'silent phenotypes' in a range of organisms including man (Nicholson *et al*, 2002; Dunn *et al*, 2005).

In this study, the interactions between systemic metabolism, loss of PPAR-α and the age of the animal have been investigated by a metabolomic investigation of the PPAR-α-null mouse fed *ad libitum* based on ^{1}H nuclear magnetic resonance (NMR) and gas chromatography-mass spectrometry (GC-MS) in conjunction with multivariate statistics. This approach has demonstrated a profound age-dependent steatosis and loss of glycogen in the liver as well as altered fatty acid metabolism in a number of tissues in the PPAR-α-null mouse. The method also provides a template for other metabolomic studies to investigate how age and genotype interact to produce a given metabolic profile.

Results

Loss of PPAR-α function results in severe perturbations in glycolysis/gluconeogenesis

The metabolic deficits of the PPAR-α-null mouse were most evident in the liver where PPAR-α expression is highest in the mouse. Using ^{1}H-NMR spectroscopy, tissue had a decreased glucose concentration relative to age-matched controls at all time points (Figure 1A). By 13 months, the glucose concentration in the PPAR-α-null mice was 12.0 ± 2.0% of that of the 3 month PPAR-α-null mice, and 15.2 ± 1.4% of that in age-matched controls. Subsequent application of PCA to all PPAR-α-null data (3–13 months) demonstrated that this effect, associated with ageing, was the dominant trend in the overall data set (Figure 1B) and the reduction in glucose becomes more pronounced with age (Figure 1C and D). This reduction in glucose is also accompanied by a significant decrease in glycogen concentration (Figure 1D). Using partial least squares (PLS) to model the metabolic changes associated with ageing in the NMR spectroscopy data set of aqueous extracts from the liver tissue, a robust predictive model was produced for the control group ($R^2(X)$=0.22; $R^2(Y)$=0.72; Q^2=0.70 for the first component; Figure 1E). This model passed cross-validation according to random permutation of the *Y* variable (age) (Figure 1F). The correlation between these metabolic changes and age were robust enough to allow the prediction of the age of individual animals according to their liver tissue metabolic fingerprints (Figure 1G). However, using the same model to predict the age of the PPAR-α-null mice from their liver tissue profiles as measured by NMR spectroscopy of the aqueous extracts demonstrated that the 13-month-old animals were predicted to be significantly older ($P<0.001$; Student's *t*-test between predicted age of wild-type and mutant mice) and in general PPAR-α-null mice were fitted to be above the line of the control mouse data. Reversing this analysis, control animals were predicted to be younger than their actual age according to a PLS model based on the metabolic changes detected in the liver tissue of PPAR-α-null mice (data not shown). The ageing trends for both mouse genotypes were associated with decreases in glucose (δ 3.46–3.90), leucine and isoleucine (δ 0.94–1.02) and increases in fatty acids (δ 1.26–1.30); lactate (δ 1.30–1.34); choline/phosphocholine (δ 3.20) and taurine (δ 3.24).

GC-MS analysis of the liver tissue also demonstrated that the liver from younger mice (3 and 5 months) could be characterised by a decrease in the number of disaccharide molecules relative to the control samples. Under conditions of low glucose/glycogen, it is known that lactate and amino acids represent important hepatic gluconeogenic substrates. As the PPAR-α-null mouse ages, there is a significant age-related increase in the number of amino acids in the liver, including alanine, aspartate and glutamate, as well as a significant increase in lactate (Figure 1H).

Analysis of other tissues revealed that the diaphragm, white adipose tissue (WAT), heart and soleus skeletal muscle from the PPAR-α-null mouse also demonstrated a decrease in the concentration of glucose, which becomes more pronounced with age, being most notable at 11–13 months (Figure 1I). In these tissues, robust PLS models were also built of the age-related changes detected in the aqueous extracts as determined by NMR spectroscopy (Figure 1J and K for diaphragm and soleus and Supplementary Figures 1 and 2 for adipose and heart). Ageing in the animals induced a decrease in glucose and glycogen in muscle tissue with the most robust models in the diaphragm and soleus muscle. However, differences between genotypes were less apparent in these PLS models when compared with the analogous model produced for the liver.

Fatty acid metabolism is affected by the loss of PPAR-α function

By 13 months, both GC-MS and ^{1}H-NMR spectroscopy indicated fatty acid accumulation in the liver. Figure 2A shows the increase in resonances corresponding to fatty acids in the ^{1}H-NMR spectrum of 13-month liver tissue relative to age-matched control tissue. Although this represents only a partial partition of the more water-soluble free fatty acids, as determined by subsequent GC-MS analysis, these fats were consistently increased in the extracts from PPAR-α-null mice. GC-MS analysis of the fatty acid content of the total lipid extracts of 13-month PPAR-α-null mice livers in conjunction with PLS-DA revealed that there was a large increase in linoleic acid (18:2), oleic acid (18:1) and di-homo-γ-linolenic acid (20:3) (Figure 2B; R^2=0.88, Q^2=0.45). As these models were formed from a relatively small number of biological repeats, the analysis was also repeated using the Student's *t*-test with a

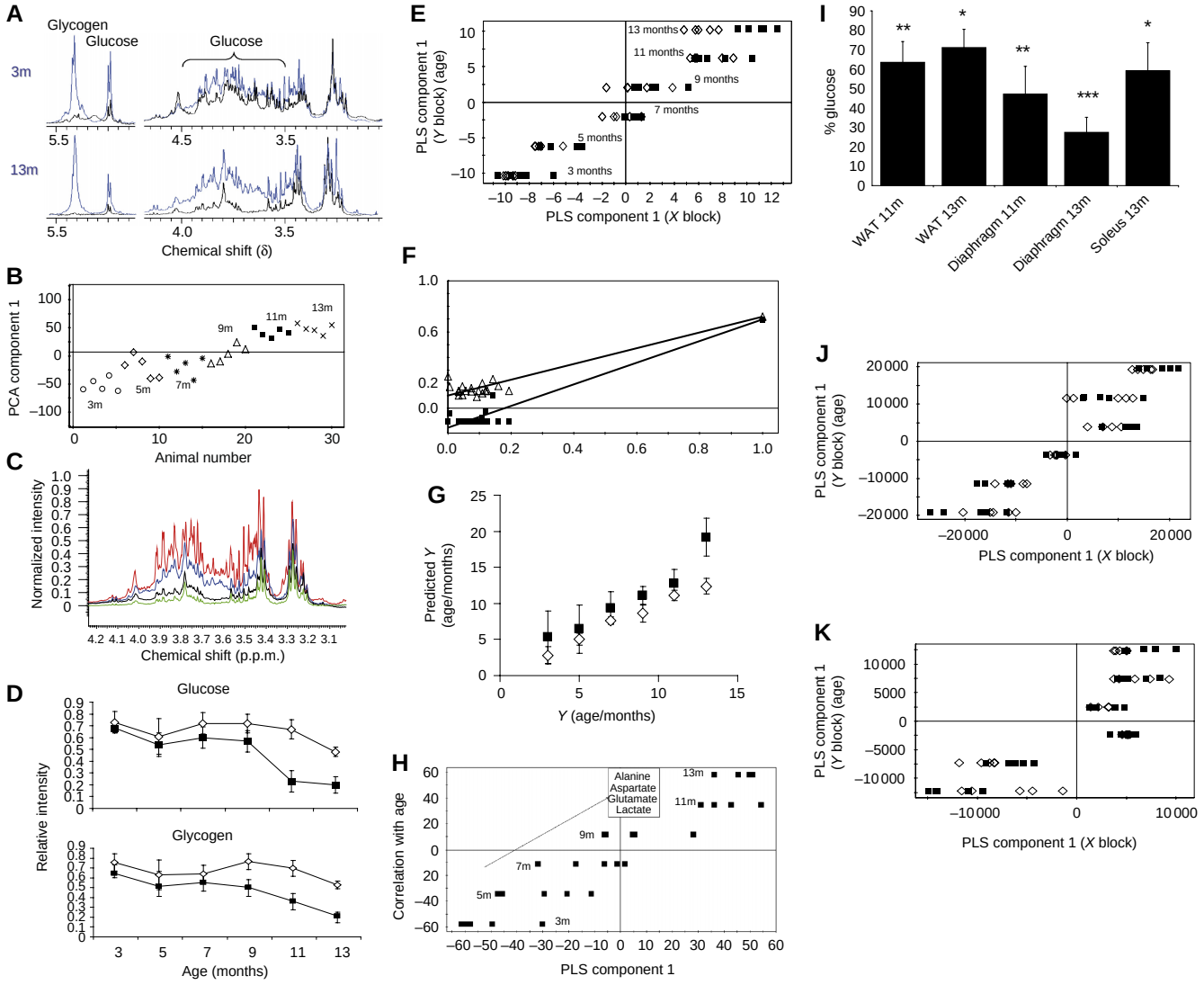

Figure 1 (**A**) ^{1}H-NMR spectra showing the difference in glucose and glycogen concentration between PPAR-α-null liver tissue samples (black) and controls (blue) at 3 and 13 months. (**B**) PCA plot showing the clusterings of 3m (open circles), 5m (open diamonds), 7m (stars), 9m (open triangles), 11m (black squares) and 13m (crosses) liver tissue across principal component 1. Note the *x*-axis is the order of samples in terms of age and does not represent a principal component. (**C**) ^{1}H-NMR spectra showing the difference in glucose and glycogen concentration between 3 and 13 months for liver tissue extracts from PPAR-α-null mice. Each spectrum is the average of the five spectra obtained from all animals at that age. Key: red, 3 months; blue, 5 months; black, 11 months; green, 13 months. (**D**) peak area of the anomeric ^{1}H α-glucose (δ 5.24) and glycogen (δ 5.40) for spectra from the extracts of liver tissue from PPAR-α-null mice (■) and control mice (◇) (**E**) PLS plot regressing age of animal (*y*-axis) against the metabolic profile of the liver tissue (*x*-axis) in control mice as measured by ^{1}H-NMR spectroscopy. PPAR-α-null mice were then mapped on to the same model. (**F**) Validation plot of PLS model in (E). Triangles predict the R^2 score and filled squares are Q^2 scores. Values to the right were the actual values for the PLS model, whereas those on the left were formed by random permutation of the *Y* variable. (**G**) Predicted age compared with actual age for a PLS plot regressing age of the animal against the metabolic profile of the liver tissue in control mice as measured by ^{1}H-NMR spectroscopy. PPAR-α-null mice were then mapped on to the same model. Each point represents the mean ± standard deviation. (**H**) PLS plot showing the age-related perturbations in aqueous soluble metabolites occurring in the PPAR-α-null liver (3–13 months) measured by GC-MS with corresponding significant metabolic changes annotated. (**I**) Percentage glucose in selected PPAR-α-null tissues relative to age-matched control tissues (error bars represent standard error) $^{*}P<0.05$; $^{**}P<0.01$; $^{***}P<0.001$. (**J**) PLS plot showing the age-related perturbations in aqueous soluble metabolites occurring in diaphragm tissue from PPAR-α-null and control mice (3–13 months) measured by NMR spectroscopy. (**K**) PLS plot showing the age-related perturbations in aqueous soluble metabolites occurring in soleus tissue from PPAR-α-null and control mice (3–13 months) measured by NMR spectroscopy. Key for all panels: ◇ control mice; ■ PPAR-α-null mice.

Bonferroni correction (Supplementary Table 7). The changes in oleic acid and di-homo-γ-linolenic acid were also detected in younger mice. Applying PLS-DA to the entire fatty acid data set produced a model with five components that separated the wild-type and PPAR-α-null mice (R^2=0.80; Q^2=0.61; Figure 2C). On examining the loadings plot for component 1, the PPAR-α-null mice showed increased concentrations of oleic acid (18:1), linoleic acid (9c, 12c-18:2) and arachidonic acid (20:4) as determined by those fatty acids that contributed significantly to the loadings plot ($P<0.05$ for each metabolite according to a jack knifing procedure). Given that the separation was over five components, the variable importance to projection (VIP) scores were also considered. VIPs examine the contribution made to the model by each variable over all

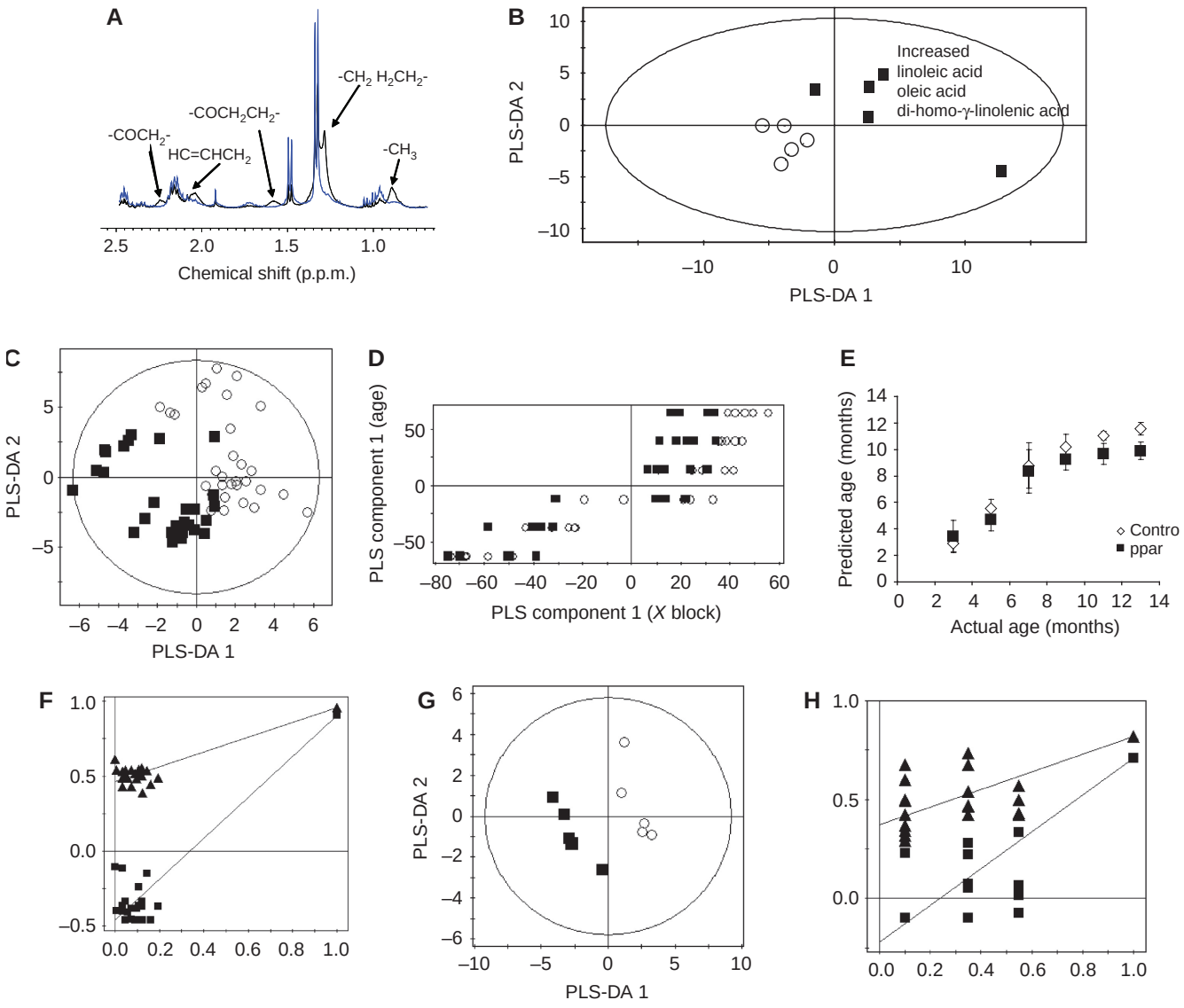

Figure 2 (**A**) A section of ^{1}H-NMR spectra (δ 0.5–2.7) showing an increase in resonances corresponding to fatty acid moieties in 13-month PPAR-α-null liver tissue (black) relative to age-matched control tissue (grey). (**B**) PLS-DA plot showing the clustering of 13-month PPAR-α-null liver samples (■) from controls (○) for the fatty acids detected by GC-MS. The corresponding significant metabolite changes are labelled. (**C**) PLS-DA plot of the fatty acids analysed by GC-MS for the entire liver tissue (key as in (C)). (**D**) A PLS plot of the regression between the fatty acid profile (as measured along the *x*-axis) and the age of the animal (*y*-axis) (key as in (C)). (**E**) Predicted age versus actual age for the PLS model in (D). Each point represents the mean ± standard deviation. (**F**) Validation plot of PLS model in (E). Filled triangles predict the R^2 score and filled squares are Q^2 scores. Values to the right were the actual values for the PLS model, whereas those on the left were formed by random permutation of the *Y* variable. (**G**) PLS-DA of free fatty acid profiles in the liver tissues from PPAR-α-null and control mice at 3 months of age. (**H**) Validation of PLS-DA model in (G).

five components. The three fats that drove the separation in PLS component 1 were also the three fats with the highest VIP score and were also deemed to be significant according to jack knifing cross-validation of their VIP scores. In a similar manner, orthogonal-PLS produced similar results (data not shown).

Applying PLS to the fatty acid profile for the liver tissue to examine the metabolic changes that accompany ageing produced a robust model for the combined data set (three components; $R^2Y=0.96$; $Q^2=0.90$; Figure 2D). This linear trend with age was associated with increases in the relative concentrations of palmitic acid (16:0) and arachidonic acid (20:4) and decreases in oleic acid (18:1) and cholesterol as the animals' age. This model robustly predicted age when wild-type and null mice were compared together between 3 and 9 months (Figure 2E). However, at 11–13 months the predicted age of the null mice was significantly lower ($P<0.01$ according to the Student's *t*-test comparing the two predicted ages for wild-type and mutant mice) for the PPAR-α-null mouse. In part, this reflects the relative increase in hepatic oleic acid in the PPAR-α-null mouse compared with wild types at any one time point, and hence this fatty acid being relatively less affected by the decrease associated with ageing. This model passed cross-validation according to random permutation of

the *Y* variable (age) (Figure 2F). Similar results were obtained when PLS models were built for the PPAR-α-null mice or the wild-type mice alone (data not shown).

As the fatty acid methyl ester analysis focused on total fatty acids found within a tissue, the free fatty acid profile of the liver was also investigated using MSTFA to derivatise free fatty acids and cholesterol derivatives prior to analysis by GC-MS. Analysis using PLS-DA robustly discriminated PPAR-α-null mice at 3 and 5 months of age (3 months, $R^2(X)=0.78$, $Q^2=0.88$; 5 months, $R^2(X)=0.78$, $Q^2=0.60$; Figure 2G and H). For both time points, this was characterised by increases in stearate and heptadecanoic acid and decreases in oleic acid and cholesterol. Although no models could be built for the data obtained from 7- and 9-month-old animals, 11 and 13 month groups could be distinguished (11 months, $R^2(X)=0.41$, $Q^2=0.41$; 13 months, $R^2(X)=0.82$, $Q^2=0.51$; data not shown). For these older animals, PPAR-α-null mice were characterised by increased free oleic acid, linoleic acid and decreased palmitic acid.

Figure 3A shows the differentiation of heart samples from PPAR-α-null mice from controls by PLS-DA for all samples regardless of age ($R^2=0.83$, $Q^2=0.52$) (Supplementary Table 2). Again, increases in oleic acid and linoleic acid were important discriminators for heart tissue from the null mice, as well as decreases in tetracosanoic acid (24:0), palmitic acid (16:0), docosahexanoic acid (22:0) and arachidonic acid (20:4). These metabolites similarly classified null from wild-type mice when considering individual age groups from 3 to 13 months (data not shown).

WAT samples from the PPAR-α-null mice were differentiated from control samples regardless of age by PLS-DA (Figure 3B; $R^2=0.77$, $Q^2=0.48$; Supplementary Table 3). The separation was attributed to increased concentrations of eicosadienoic acid (20:2), eicosanoic acid (20:0), tridecanoic acid (13:0), docosadienoic acid (22:2), di-homo-γ-linolenic acid (20:3) and hexadecadienoic acid (16:2), and decreased concentrations of octadecanoic acid (18:0), heptadecanoic acid (17:0), hexadecenoic acid (16:1) and tetradecenoic acid (14:1).

Using PLS analysis to examine ageing metabolic trends in the PPAR-α-null WAT, there was a significant age-related increase in a number of saturated fatty acids including stearic acid (18:0), palmitic acid (16:0), tetradecanoic acid (14:0) and heptadecanoic acid (17:0), as well as a decrease in docosahexaenoic acid (22:6), which is the β-oxidation product of tetracosahexaenoic acid (24:6) (Figure 3C). However, these changes were similarly detected in the wild-type animals and therefore were not a direct result of PPAR-α deletion but were associated with normal metabolic changes associated with ageing.

Loss of PPAR-α function causes significant metabolic perturbations in muscle tissue

The soleus and gastrocnemius were investigated to compare and contrast type I (oxidative; soleus) and mixed type I/type II (gastrocnemius) muscles by GC-MS (Supplementary Figure 3a) and NMR (Supplementary Figure 3b). Analysis of

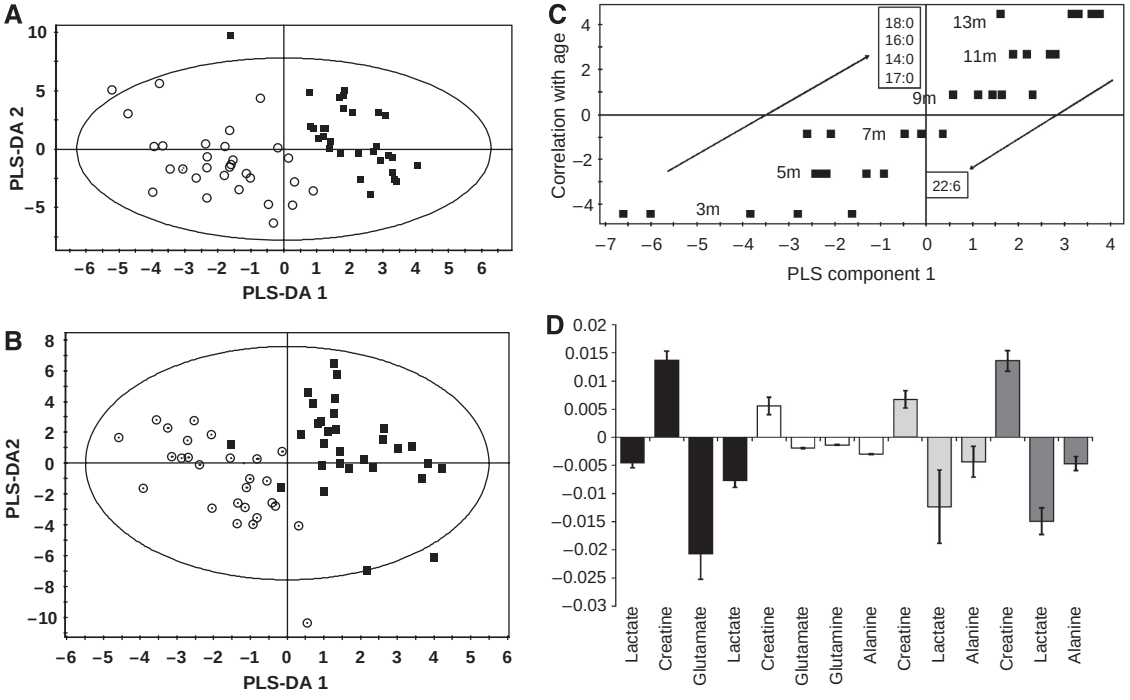

Figure 3 PLS-DA plots showing the differentiation of 3–13 month PPAR-α-null (■) and control (○) samples in (**A**) heart tissue and (**B**) white adipose tissue following methyl esterification of the fatty acid complement, and analysis by GC-MS. (**C**) PLS plot showing the age-related perturbations in lipid metabolites occurring in the PPAR-α-null WAT (3–13 months) with corresponding significant metabolic changes annotated. (**D**) PLS coefficient values showing the contribution of selected metabolites to age-related metabolic trends in the gastrocnemius, soleus, heart and diaphragm in the PPAR-α-null mouse. All coefficients shown are significant at the 95% confidence limit. Error bars indicate standard error.

the soleus muscle from the PPAR-α-null mice demonstrated an increased concentration of lactate and a decreased concentration of creatine at all time points examined. In the gastrocnemius, increased concentrations of alanine and lactate and a decreased concentration of creatine characterised the null mouse (data not shown).

PLS analysis of both the soleus and gastrocnemius muscle from the PPAR-α-null mouse showed a significant age-related increase in creatine concentration, and a concomitant decrease in lactate and glutamate in both tissues, as well as additional decreases in alanine and glutamine in the soleus only (Figure 3D). Similar perturbations were also observed in the heart and diaphragm; the concentration of creatine increased, whereas alanine and lactate concentrations decreased significantly with age in these tissues (Figure 3D). Interestingly, the soleus muscle also showed an age-related increase in the concentrations of stearic acid (18:0) and palmitic acid (16:0) (data not shown).

GC-MS analysis of the heart also showed a reduction in β-hydroxybutyrate, a ketone body used to supply energy to the heart under conditions of low glucose intake. This reduction was evident at 5 and 9 months (data not shown). A complete list of the most significant changes is available as part of the online Supplementary Tables 1–9 and summarised in Figure 4.

Discussion

Differential expression of genes encoding enzymes involved in mitochondrial and peroxisomal fatty acid oxidation constitutes well-characterised alterations in the PPAR-α-null mouse (reviewed in Mandard *et al*, 2004). Despite this, previous studies on this mouse have largely reported no obvious phenotype unless fasted, under which conditions the defects in fatty acid oxidation, gluconeogenesis and ketogenesis result in an increase in the concentration of circulating free fatty acid levels, hypoglycaemia, hypoketonaemia and hypothermia (Djouadi *et al*, 1998; Kersten *et al*, 1999; Leone *et al*, 1999), or under high fat feeding conditions where the heart has decreased myocardial fatty acid oxidation and some evidence of age-related cardiomyopathy (Watanabe *et al*, 2000). In this study, we demonstrate that the unchallenged PPAR-α-null mouse fed *ad libitum* possesses underlying perturbations in metabolism, which are attributable to reduced glucose and glycogen storage in the liver and alterations in the metabolism of fatty acids. We also identified a number of metabolic changes associated with ageing in both mouse genotypes and these either exacerbated or reduced the effects of genetic modification as the PPAR-α-null mice aged.

To examine ageing trends in both mouse genotypes, the multivariate statistical approach of PLS was used. This algorithm determines the linear (or polynomial) correlation between a dependent variable or variables (Y) and a matrix of predictor variables (X). In this study, we have used this approach to determine the metabolic changes associated with ageing in both wild-type and PPAR-α knockout mice. These trends were robust enough to predict the age of the animal from the metabolic profiles of the tissue being examined for the liver, muscle and heart tissue. Furthermore, by producing models from tissues of wild-type animals only, the profiles of tissue from the PPAR-α-null mice can be examined to see whether these ageing trends are also present. In the liver tissue, regardless of genotype, ageing was characterised by a decrease in glucose and glycogen in the aqueous extracts and increases in palmitic acid (16:0) and arachidonic acid (20:4) and decreases in oleic acid (18:1) and cholesterol in the lipid extracts. However, although these metabolic changes could be used to age animals according to the metabolic profiles of their tissues, it is important to stress that deviations from the trend do not mean that the ageing process in an animal is either increased or decreased. Rather this process has detected an interaction between the metabolic changes that accompany ageing and those that accompany the genetic modification.

In addition to the decrease in liver glucose and glycogen detected by PLS in both mouse strains with age, metabolic changes detected in the liver of PPAR-α-null mice are consistent with reduced glucose storage and production by gluconeogenesis. The combination of these effects resulted in

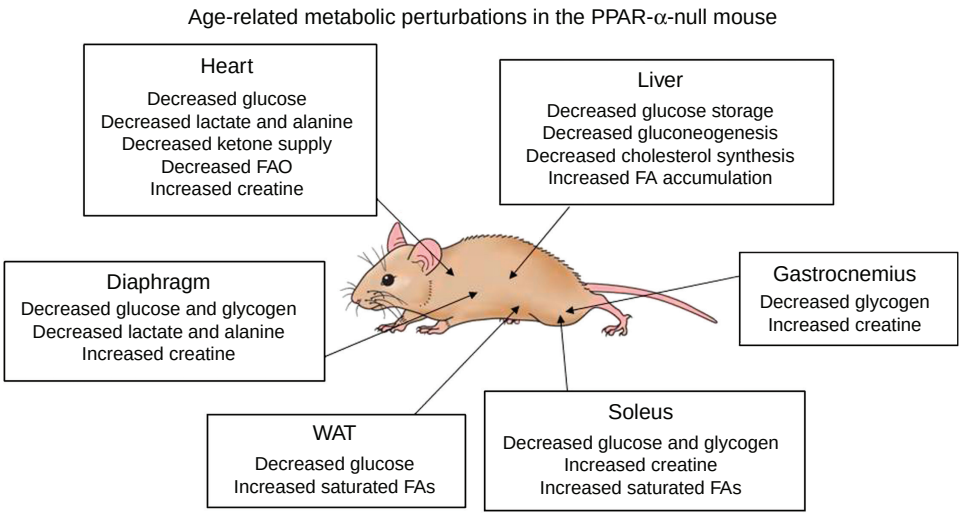

Figure 4 A summary figure of the key changes between wild-type and PPAR-α-null mice and associated with ageing in both mouse genotypes.

the development of a hypoglycaemic state in older PPAR-α-null mice, similar to that induced by fasting in the younger mouse, where liver glucose and glycogen were markedly reduced. Under conditions of low hepatic glycogen concentrations, as observed here in the older mice, the liver may use lactate and amino acids such as alanine and glutamine for continued glucose biosynthesis (Kaloyianni and Freedland, 1990). In this study, we observed an age-related increase in hepatic alanine and lactate concentrations which suggest that, although these gluconeogenic precursors are present in the liver, there is a failure to convert them to glucose, which is most likely to be a consequence of the reduced glucose-6-phosphatase (*G6pc*) and phosphoenolpyruvate carboxykinase 1 (*Pck1*) expression (see below and Supplementary information). This effect in turn is likely to exacerbate the hypoglycaemia observed in the ageing PPAR-α-null mouse. Xu *et al* (2002) have previously investigated impaired gluconeogenesis in the liver in young (4 month old) mice under fed and fasted conditions, demonstrating a reduction in the production of glucose from lactate under both conditions.

To further characterise the reduction in gluconeogenesis, RT–PCR was performed to measure the expression of key genes involved in this pathway (Supplementary information). Consistent with reduced gluconeogenesis, we observed a 2.7-fold reduction in the transcription of *G6pc*, and a 5-fold reduction in *Pck1*, the latter exerting a high degree of metabolic control over the gluconeogenic pathway. *G6pc* expression is in part controlled by PPAR-γ coactivator 1 (*Ppargc1a*) (Soyal *et al*, 2006), which was also reduced two-fold. The perturbation in glucose flux may in turn also account for the reduced expression of 6-phosphofructo-2-kinase/fructose-2,6-biphosphatase (*Pfkf3b*), a key enzyme in the control of glycolysis and gluconeogenesis.

There was a concomitant age-related decrease in lactate in all muscle tissues analysed, and alanine in the soleus, heart and diaphragm. The concentration of glucose was also seen to decrease significantly in an age-dependant manner in both the soleus and diaphragm. Taken together, these findings are consistent with a reduction in glycolysis in muscle tissue. Interestingly, the soleus muscle also showed an age-related increase in stearic acid and palmitic acid concentrations. Unlike the gastrocnemius, which is composed of both type I (oxidative) and type II (glycolytic) muscle fibres, the soleus is composed solely of type I muscle fibres, which primarily stores fuel in the form of triglyceride.

Fatty acids represent an alternative energy source, which allows glucose to be spared for tissues such as brain that are unable to metabolise significant amounts of fatty acids. In the liver, fatty acids can be metabolised ultimately through the TCA cycle to generate ATP, or can be used for ketogenesis. As PPAR-α controls the expression of many enzymes involved in both the β-oxidation and ketogenic pathways, fatty acids accumulate in the livers of PPAR-α-deficient mice (Hashimoto *et al*, 2000). An age-related accumulation of fatty acids was detected in the livers of the PPAR-α-null mice by both NMR spectroscopy and GC-MS. Patsouris *et al* (2006) have previously reported an increase in hepatic triglyceride in PPAR-α-null mice. However, when considering the total fatty acid complement of the liver tissue, the major fatty acid changes that characterised the PPAR-α-null mouse were also fatty acids that changed during the normal process of ageing. In particular, oleate was increased in the livers of PPAR-α-null mice at individual time points, but it also decreased with age. In contrast to the changes we detected in the aqueous metabolite complement of liver tissue, the net effect of these two metabolic perturbations in lipid metabolism in the liver were that the 13-month-old PPAR-α-null mice appeared to be younger than their wild-type controls when aged through their lipid profiles. Oleate increases in the liver of the PPAR-α-null mouse because several of the enzymes involved in the subsequent metabolism of this fatty acid, including the elongases, Elovl-5 and -6, and the Δ5 and Δ6 desaturases, which produce polyunsaturated fats such as arachidonic acid, are partly under the regulation of PPAR-α. Oleate is also found in high concentrations in liver TAGs, suggesting that the observed steatosis may be exacerbated by the increased oleate found in the PPAR-α-null mouse.

Analysis of fatty acids using fatty acid methyl esterification produces a data set reflecting the total fatty acid complement of a tissue. Although for many tissues this reflects triglyceride deposits it will also be influenced by cell membrane and non-esterified free fatty acids. In the liver, NEFAs and cholesterol derivatives were also measured. This approach produced some interesting differences compared with the total fatty acid complement with young PPAR-α-null mice being characterised by a decreased oleate/stearate ratio, in keeping with the fact that stearoyl-CoA desaturase (SCD) is in part under PPAR-α control. Furthermore, cholesterol was also decreased in young PPAR-α-null mice and again cholesterol synthesis is in part regulated by PPAR-α, particularly with respect to diurnal variation in cholesterol synthesis (Patel *et al*, 2001). No difference was found in mice between 7 and 9 months of age but at 11–13 months of age again PPAR-α-null mice were distinguished by their free fatty acid profile, but this time by increased oleic acid, linoleic acid and decreased palmitic acid. The increase in oleic acid now mirrored the global increase detected in this fatty acid, suggesting that this change was now determined by the accumulation of triglyceride in the liver rather than which enzymes were under PPAR-α control.

Hearts of the PPAR-α-null mice exhibited signs of perturbed energy homoeostasis associated with a reduced supply of ketone bodies. Heart tissue from the PPAR-α-null mouse had decreased β-hydroxybutyrate, reflecting the well-documented decline in ketogenesis (Kersten *et al*, 2000; Barak and Kim, 2007). As evidence of perturbed fatty acid synthesis in the PPAR-α-null mouse, there was a consistent increase in linoleic acid, and a decrease in arachidonic acid at the majority of time points studied. Linoleic acid is converted to arachidonic acid through elongases and desaturases, enzymes the expression of which are partly under the control of PPAR-α (Wang *et al*, 2006).

The metabolomic analysis of the WAT revealed an increase in the concentration of several saturated fatty acids with age consistent with a reduction in SCD activity, the expression of which is, in part, controlled by PPAR-α (Wang *et al*, 2006). However, these changes occurred in the WAT of both null and wild-type mice, indicating that the reductions in SCD activity occur as part of the normal ageing process, and may actually be the result of an age-related decrease in PPAR-γ expression (Ye *et al*, 2006) which, in part, controls the expression of SCD

(Riserus *et al*, 2005), and is much more abundantly expressed in adipose tissue than PPAR-α (Braissant *et al*, 1996).

In conclusion, our metabolomic study demonstrates that a loss of PPAR-α results in a marked reduction in hepatic glucose/glycogen and subsequent hepatic steatosis with age. This is also accompanied by decreased glucose metabolism and a reduction in the synthesis of polyunsaturated fats across the whole organism. These changes interact with the normal metabolic changes that accompany ageing, which either magnify or diminish the metabolic perturbations detected, demonstrating that the study of any genetic modification should be placed in context with the normal ageing process.

Materials and methods

Tissue collection

All animal procedures conformed to the guidelines determined by the UK Home Office for animal welfare. Tissues from wild-type SVEV/129 mice and PPAR-α-null mice were obtained from stable colonies at the University of Oxford (n=5; 3, 5, 7, 9, 11 and 13 months age). Mice were fed standard laboratory chow *ad libitum* prior to death (Special Diet Services, Essex, UK). Mice were injected subcutaneously with a 0.3 ml mixture of medetomidine (10%; Pfizer Limited, Kent, UK), ketamine (7.6%; Vétoquinol UK Limited, Bicester, UK) in sterile water, and tissue collection was performed after the loss of corneal and pedal reflexes. Abdominal WAT, hearts, livers, skeletal muscle (gastrocnemius and soleus) and diaphragms were rapidly dissected (<60 s post-mortem time prior to freezing), frozen in liquid nitrogen and stored at −80°C.

Metabolomics analyses

Tissues were extracted using a methanol–chloroform–water extraction procedure to separate aqueous-soluble metabolites from lipids as described previously (Atherton *et al*, 2006). Briefly, ∼100 mg tissue were pulverised with dry ice. Here, 600 μl methanol–chloroform (2:1) was added and the samples were sonicated for 15 min. Water and chloroform were added (200 μl of each) and the samples were centrifuged for 20 min. The resulting aqueous and organic layers were separated from the protein pellet. The organic layer was dried overnight in a fume hood, whereas the aqueous extracts were evaporated to dryness using an evacuated centrifuge (Eppendorf, Hamburg, Germany).

NMR spectroscopy

The dried aqueous extracts were rehydrated in 600 μl D_2O, buffered in 0.24 M sodium phosphate (pH 7.0) containing 1 mM (sodium-3-(trimethylsilyl)-2,2,3,3-tetradeuteriopropionate (TSP) (Cambridge Isotope Laboratories Inc., Andover, MA, USA) as an internal standard. The samples were analysed using an INOVA spectrometer operating at 400.13 MHz for the ^{1}H frequency (Varian, CA, USA) using a 5-mm broadband inverse probe. Spectra were collected using a solvent suppression pulse sequence based on a one-dimensional NOESY pulse sequence to saturate the residual ^{1}H water proton signal (relaxation delay=2 s, t_1=3 μs, mixing time=150 ms, solvent presaturation applied during the relaxation time and the mixing time). In total, 128 transients were collected into 16K data points over a spectral width of 12 p.p.m. at 37°C. For this assay, the coefficients of variation for various metabolites detected in the extracts of liver tissue are shown in the Supplementary information.

GC-MS

Aqueous samples were derivatised using the procedure reported by Gullberg *et al* (2004). An aliquot of 150 μl of the D_2O sample used for ^{1}H-NMR spectroscopy was evaporated to dryness in an evacuated centrifuge and 30 μl methoxyamine hydrochloride (20 mg ml^{-1} in pyridine) was added. The samples were vortex mixed for 1 min, and derivatised at room temperature for 17 h. Samples were then silylated with 30 μl of *N*-methyl-*N*-trimethylsilyltrifluoroacetamide for 1 h at room temperature. The derivatised samples were diluted (1:10) with hexane prior to GC-MS analysis.

Organic-phase metabolites were derivatised by acid catalysed esterification (Morrison and Smith, 1964). Lipids were dissolved in 0.25 ml of chloroform/methanol (1:1 v/v). An aliquot of 0.10 ml BF_3/methanol (Sigma-Aldrich) was added and the vials were incubated at 80°C for 90 min. Once cool 0.3 ml H_2O (mQ) and 0.6 ml hexane were added and each vial was vortex mixed for 1 min. The aqueous layer was discarded and the remaining organic layer was evaporated to dryness before reconstitution in 200 μl hexane for analysis.

The derivatised aqueous samples were injected into a Thermo Electron Trace GC Ultra equipped with a 30 m × 0.25 mm ID 5% phenyl polysilphenylene-siloxane column with a chemically bonded 25 μm TR-5MS stationary phase (Thermo Electron Corporation; injector temperature=220°C, helium carrier gas flow rate=1.2 ml min^{-1}). The initial column temperature was 70°C; this was held for 2 min and then increased by 5°C min^{-1} to 310°C and was held for 20 min.

The derivatised organic metabolites were injected onto a ZB-WAX column (30 m × 0.25 mm ID × 0.25 μm df; 100% polyethylene glycol). The initial column temperature was 60°C; this was held for 2 min and then increased by 10°C min^{-1} to 150°C and then by 4°C min^{-1} up to a temperature of 230°C where it was held for 7 min.

The column eluent was introduced into a DSQ quadrupole mass spectrometer (Thermo Electron Corporation) (transfer line temperature=310°C for aqueous metabolites and 240°C for lipid metabolites, ion source temperature=250°C, electron beam=70 eV). The detector was turned on after a solvent delay of 240 s and data were collected in full-scan mode using three scans per second across a mass range of 50–650 m/z. For this assay, the coefficients of variation for various fatty acids are shown in the Supplementary information.

Data analysis

NMR spectra were processed using ACD SpecManager 1D NMR processor (version 8; ACD, Toronto, Canada). Spectra were Fourier transformed following multiplication by a line broadening of 1 Hz, and referenced to TSP at 0.0 p.p.m. Spectra were phased and baseline corrected manually. Each spectrum was integrated using 0.04 p.p.m. integral regions between 0.5–4.5 and 5.1–10.0 p.p.m. To account for any difference in concentration between samples, each spectral region was normalised to a total integral value of 10 000.

GC-MS chromatograms were analysed using Xcalibur (v. 2.0; Thermo Fisher Corp.), integrating each peak individually. Peaks were normalised so that the total sum of peaks was set to 10 000. Deconvolution of overlapping peaks was achieved by generating traces of selected ions. A 0.1-min threshold window was used for the deviation of peaks away from the predicted retention time across the data set. Structures were assigned using both the NIST database of mass spectra and analysis of standard compounds.

Data sets were imported into SIMCA-P 10.0 (Umetrics, Umeå, Sweden) for processing using PCA, PLS (a regression extension of PCA used to separate out a trend from other variation in the data set) and PLS-DA (a regression extension of PCA used for classification). Identification of major metabolic perturbations within the pattern recognition models was achieved by the analysis of corresponding loading plots. PLS plots were used to identify variations correlated with age. Additionally, R^2 and Q^2 were used as measures for the robustness of a pattern recognition model. R^2 is the fraction of variance explained by a component, and cross-validation of R^2 gives Q^2, which reveals the fraction of the total variation predicted by a component. Both values are indicative of how good the overall model is. Typically, a robust model has $R^2>0.50$ and $Q^2>0.40$. Coefficient scores rank the observations according to their contribution to the model. To confirm which metabolites contributed significantly to each model, each variable was assessed by a jack-knifing routine to assess its contribution to a given component. Only

variables deemed to have a coefficient significantly different from zero were included.

The overall strategy for data analysis was as follows. Metabolite differences at a given age were determined by producing a PLS-DA plot comparing wild-type and null mice and taking those metabolites that made a significant contribution to the first PLS-DA component provided that the model was deemed to have a sufficiently robust Q^2 (>0.40). In addition, PLS was used to regress the age of the animal against the metabolic profile for that tissue. This was performed on both wild-type and null mice.

Supplementary information

Supplementary information is available at the *Molecular Systems Biology* website (www.nature.com/msb).

Conflict of interest

The authors declare competing financial interests.

Acknowledgements

We thank Frank Gonzalez (NIH) for the kind gift of PPAR-α null mice. This study was supported by grants from the British Heart Foundation (to KC and JLG; PG/05/081), the Wellcome Trust (JLG; 072829/Z/03/Z), the BBSRC and Selcia Ltd. (HJA and JLG). JLG is a member of The MRC Centre for Obesity and related Metabolic Diseases.

References

Atherton HJ, Bailey NJ, Zhang W, Taylor J, Major H, Shockcor J, Clarke K, Griffin JL (2006) A combined ^{1}H-NMR spectroscopy- and mass spectrometry-based metabolomic study of the PPAR-alpha null mutant mouse defines profound systemic changes in metabolism linked to the metabolic syndrome. *Physiol Genomics* **27:** 178–186

Barak Y, Kim S (2007) Genetic manipulations of PPARs: effects on obesity and metabolic disease. *PPAR Res* **2007:** 12781

Berger J, Moller DE (2002) The mechanisms of action of PPARs. *Annu Rev Med* **53:** 409–435

Braissant O, Foufelle F, Scotto C, Dauca M, Wahli W (1996) Differential expression of peroxisome proliferator-activated receptors (PPARs): tissue distribution of PPAR-alpha, -beta, and -gamma in the adult rat. *Endocrinology* **137:** 354–366

Desvergne B, Wahli W (1999) Peroxisome proliferator-activated receptors: nuclear control of metabolism. *Endocr Rev* **20:** 649–688

Djouadi F, Weinheimer CJ, Saffitz JE, Pitchford C, Bastin J, Gonzalez FJ, Kelly DP (1998) A gender-related defect in lipid metabolism and glucose homeostasis in peroxisome proliferator-activated receptor alpha-deficient mice. *J Clin Invest* **102:** 1083–1091

Dreyer C, Krey G, Keller H, Givel F, Helftenbein G, Wahli W (1992) Control of the peroxisomal beta-oxidation pathway by a novel family of nuclear hormone receptors. *Cell* **68:** 879–887

Dunn WB, Bailey NJ, Johnson HE (2005) Measuring the metabolome: current analytical technologies. *Analyst* **130:** 606–625

Griffin JL (2004) Metabolic profiles to define the genome: can we hear the phenotypes? *Philos Trans R Soc Lond B Biol Sci* **359:** 857–871

Guerre-Millo M, Gervois P, Raspe E, Madsen L, Poulain P, Derudas B, Herbert JM, Winegar DA, Willson TM, Fruchart JC, Berge RK, Staels B (2000) Peroxisome proliferator-activated receptor alpha activators improve insulin sensitivity and reduce adiposity. *J Biol Chem* **275:** 16638–16642

Gullberg J, Jonsson P, Nordstrom A, Sjostrom M, Moritz T (2004) Design of experiments: an efficient strategy to identify factors influencing extraction and derivatization of *Arabidopsis thaliana* samples in metabolomic studies with gas chromatography/mass spectrometry. *Anal Biochem* **331:** 283–295

Hashimoto T, Cook WS, Qi C, Yeldandi AV, Reddy JK, Rao MS (2000) Defect in peroxisome proliferator-activated receptor alpha-inducible fatty acid oxidation determines the severity of hepatic steatosis in response to fasting. *J Biol Chem* **275:** 28918–28928

Iemitsu M, Miyauchi T, Maeda S, Tanabe T, Takanashi M, Irukayama-Tomobe Y, Sakai S, Ohmori H, Matsuda M, Yamaguchi I (2002) Aging-induced decrease in the PPAR-alpha level in hearts is improved by exercise training. *Am J Physiol Heart Circ Physiol* **283:** H1750–H1760

Issemann I, Prince R, Tugwood J, Green S (1992) A role for fatty acids and liver fatty acid binding protein in peroxisome proliferation? *Biochem Soc Trans* **20:** 824–827

Kaloyianni M, Freedland RA (1990) Contribution of several amino acids and lactate to gluconeogenesis in hepatocytes isolated from rats fed various diets. *J Nutr* **120:** 116–122

Keller H, Dreyer C, Medin J, Mahfoudi A, Ozato K, Wahli W (1993) Fatty acids and retinoids control lipid metabolism through activation of peroxisome proliferator-activated receptor-retinoid X receptor heterodimers. *Proc Natl Acad Sci USA* **90:** 2160–2164

Kersten S, Desvergne B, Wahli W (2000) Roles of PPARs in health and disease. *Nature* **405:** 421–424

Kersten S, Seydoux J, Peters JM, Gonzalez FJ, Desvergne B, Wahli W (1999) Peroxisome proliferator-activated receptor alpha mediates the adaptive response to fasting. *J Clin Invest* **103:** 1489–1498

Le May C, Pineau T, Bigot K, Kohl C, Girard J, Pegorier JP (2000) Reduced hepatic fatty acid oxidation in fasting PPARalpha null mice is due to impaired mitochondrial hydroxymethylglutaryl-CoA synthase gene expression. *FEBS Lett* **475:** 163–166

Lee SS, Pineau T, Drago J, Lee EJ, Owens JW, Kroetz DL, Fernandez-Salguero PM, Westphal H, Gonzalez FJ (1995) Targeted disruption of the alpha isoform of the peroxisome proliferator-activated receptor gene in mice results in abolishment of the pleiotropic effects of peroxisome proliferators. *Mol Cell Biol* **15:** 3012–3022

Leone TC, Weinheimer CJ, Kelly DP (1999) A critical role for the peroxisome proliferator-activated receptor alpha (PPARalpha) in the cellular fasting response: the PPARalpha-null mouse as a model of fatty acid oxidation disorders. *Proc Natl Acad Sci USA* **96:** 7473–7478

Mandard S, Muller M, Kersten S (2004) Peroxisome proliferator-activated receptor alpha target genes. *Cell Mol Life Sci* **61:** 393–416

Morrison WR, Smith LM (1964) Preparation of fatty acid methyl esters and dimethylacetals from lipids with boron fluoride—methanol. *J Lipid Res* **5:** 600–608

Motojima K, Passilly P, Peters JM, Gonzalez FJ, Latruffe N (1998) Expression of putative fatty acid transporter genes are regulated by peroxisome proliferator-activated receptor alpha and gamma activators in a tissue- and inducer-specific manner. *J Biol Chem* **273:** 16710–16714

Nicholson JK, Connelly J, Lindon JC, Holmes E (2002) Metabonomics: a platform for studying drug toxicity and gene function. *Nat Rev Drug Discov* **1:** 153–161

Patel DD, Knight BL, Wiggins D, Humphreys SM, Gibbons GF (2001) Disturbances in the normal regulation of SREBP-sensitive genes in PPAR alpha-deficient mice. *J Lipid Res* **42:** 328–337

Patsouris D, Reddy JK, Muller M, Kersten S (2006) Peroxisome proliferator-activated receptor alpha mediates the effects of high-fat diet on hepatic gene expression. *Endocrinology* **147:** 1508–1516

Peters JM, Hennuyer N, Staels B, Fruchart JC, Fievet C, Gonzalez FJ, Auwerx J (1997) Alterations in lipoprotein metabolism in peroxisome proliferator-activated receptor alpha-deficient mice. *J Biol Chem* **272:** 27307–27312

Riserus U, Tan GD, Fielding BA, Neville MJ, Currie J, Savage DB, Chatterjee VK, Frayn KN, O'Rahilly S, Karpe F (2005) Rosiglitazone increases indexes of stearoyl-CoA desaturase activity in humans: link to insulin sensitization and the role of dominant-negative mutation in peroxisome proliferator-activated receptor-gamma. *Diabetes* **54:** 1379–1384

Rubins HB, Robins SJ, Collins D, Nelson DB, Elam MB, Schaefer EJ, Faas FH, Anderson JW (2002) Diabetes, plasma insulin, and cardiovascular disease: subgroup analysis from the Department of Veterans Affairs high-density lipoprotein intervention trial (VA-HIT). *Arch Intern Med* **162:** 2597–2604

Sanguino E, Roglans N, Alegret M, Sanchez RM, Vazquez-Carrera M, Laguna JC (2005) Atorvastatin reverses age-related reduction in rat hepatic PPARalpha and HNF-4. *Br J Pharmacol* **145:** 853–861

Soyal S, Krempler F, Oberkofler H, Patsch W (2006) PGC-1alpha: a potent transcriptional cofactor involved in the pathogenesis of type 2 diabetes. *Diabetologia* **49:** 1477–1488

Wang Y, Botolin D, Xu J, Christian B, Mitchell E, Jayaprakasam B, Nair MG, Peters JM, Busik JV, Olson LK, Jump DB (2006) Regulation of hepatic fatty acid elongase and desaturase expression in diabetes and obesity. *J Lipid Res* **47:** 2028–2041

Watanabe K, Fujii H, Takahashi T, Kodama M, Aizawa Y, Gonzalez FJ, Aoyama T (2000) Constitutive regulation of cardiac fatty acid metabolism through peroxisome proliferator-activated receptor alpha associated with age-dependent cardiac toxicity. *J Biol Chem* **275:** 22293–22299

Weckwerth W (2003) Metabolomics in systems biology. *Annu Rev Plant Biol* **54:** 669–689

Xu J, Xiao G, Trujillo C, Chang V, Blanco L, Joseph SB, Bassillan S, Saad MF, Tontonoz P, Lee WN, Kurland IJ (2002) Peroxisome proliferator-activated receptor alpha (PPAR alpha) influences substrate utilization for hepatic glucose production. *J Biol Chem* **277:** 50237–50244

Ye P, Wang ZJ, Zhang XJ, Zhao YL (2005) Age-related decrease in expression of peroxisome proliferator-activated receptor alpha and its effects on development of dyslipidemia. *Chin Med J (Engl)* **118:** 1093–1098

Ye P, Zhang XJ, Wang ZJ, Zhang C (2006) Effect of aging on the expression of peroxisome proliferator-activated receptor gamma and the possible relation to insulin resistance. *Gerontology* **52:** 69–75

